International Journal of Applied Engineering Research ISSN 0973-4562 Volume 13, Number 1 (2018) pp. 511-519

Numerical Analysis of Vertical Motion Control of a Floating Structure with a Two-Body Interaction

Min-Jae Shin*, Weoncheol Koo*,† and Sung-Jae Kim**

**Dept. of Naval Architecture and Ocean Engineering, Inha University, Incheon, 22212, Korea.*
***School of Naval Architecture and Ocean Engineering, University of Ulsan, Ulsan, 44610, Korea.*
E-mail IDs: rosekamp@naver.com, nwavetank@gmail.com (corresponding author), slayersj8@nate.com
†Orcid: 0000-0002-4384-0996

Abstract

A numerical study on the heave reduction of a floater connected to a submerged body was conducted in the potential-flow computational domain. A two-degrees-of-freedom system was modeled to control the vertical motion of a floater and a submerged body. The drag force acting on the submerged body was applied to the equation of two-body motion to model the viscous effect. A parametric study revealed variations in the frequency of the maximum floater heave reduction according to the dimensions of the submerged body and stiffness of the connection line. Hence, a heave response amplitude operator (RAO) of the floater can be regulated by a two-body interaction. The ratios of the heave reduction were compared for various body conditions in regular waves. The optimal conditions for the maximum floater heave reduction were predicted regarding the resonant frequency of single body motion.

Keyword: Heave RAO; Vertical motion control; Two-body interaction; Drag force; Floater; Submerged body; Two-degrees-of-freedom

INTRODUCTION

Oceans provide infinite resources, such as energy, living space, and food, in addition to natural minerals that are essential for human life. Therefore, the efficient and eco-friendly development of ocean space is critical for improving the quality of human life. In recent years, the safety of coastal and marine facilities has become an important issue due to coastal erosion and flooding from natural disasters, such as sea-level rise, swells, and frequent floods caused by global climate change. In the same situation mentioned above, it is very important to design coastal structures safely for coastal and marine developments, such as marine tourism, marine leisure, and renewable energy, such as wind and wave-energy.

In general, compared to fixed structures, floating structures are more environment-friendly in coastal areas. A floater has the advantage of allowing flow exchange below the surface in the marina and the harbor areas. Floating structures, however, are vulnerable to severe fluctuations from external excitation, such as wind, waves, and current loads. The motion of a floating structure can become exceedingly aggressive when the frequency of an excitation force approaches the natural frequency of the body. In particular, the more the natural frequency of these commonly employed structures, such as a marina structure, approaches the resonance frequency, the greater is the threat to pedestrian safety and anchored boats. On the other hand, user access and boat safety is enhanced with smaller fluctuations of a floating structure.

The relative motion can be reduced by connecting a damping plate to a float that can add viscous damping or added mass. Reducing the response of floating structures in waves is necessary to the design of a safe and reliable ocean structure. To date, several methods have been studied to reduce the body fluctuations. One feasible method is to increase the level of viscous damping by installing a heave plate onto the submerged body to moderate the vertical movement of a floating structure.

Cozijn et al. (2005) conducted a forced oscillation model test of a CALM buoy with a skirt and compared the results with radiation-diffraction calculations. The quadratic damping component due to the skirt was regarded as the drag coefficient (C_D values) determined from the model test results. Tao et al. (2007) also examined a cylindrical structure with a disk type heave plate. They investigated the influence of the disk ratio on the vortex shedding pattern and associated hydrodynamic heave damping arising from the cylinder and disk.

Various studies of viscous damping with a heave plate have been reported. Tao and Cai (2004) examined the vortex-shedding flow resulting from vertical movement of a cylinder with a heave plate attached at the keel. They obtained a finite difference solution of a viscous fluid using the Navier–Stokes equations for incompressible viscous flow. Shen et al. (2012) examined the relationship between the heave plate thickness and damping force using Computational Fluid Dynamics (CFD). Geng et al. (2012) studied the viscous damping effect on the first-order motion response of a truss spar using a higher-order boundary element method (HOBEM) in the time domain. Li et al. (2013) conducted a series of experiments on the heave plates, in which they examined the effects of the KC number, oscillation frequency, plate depth, thickness-to-width ratio, shape of the edge, perforation ratio, hole size, and plate spacing.

This paper presents the results of a numerical study on the control of the natural frequency of a floating structure to minimize the floater's motion using a two-body interaction between a floater and a submerged body. Most of the studies mentioned above increased the relative motion using a submerged body to maximize the wave power. On the other hand, to the best of the authors' knowledge, little work has been done to reduce the motion of the floater with the control

of a submerged body at a target frequency.

Using an in-house developed program associated with the hydrodynamic analysis program (AQWA), the radiation and diffraction problem of two-body systems modeled together were calculated in the potential-flow computational domain. The first-order hydrostatic and hydrodynamic parameters were obtained. The program is based on the linear potential theory assuming an incompressible, inviscid, and irrotational fluid. The boundary integral equation derived from the Laplace equation was solved in the computational fluid domain. The velocity potential can then be obtained on each discretized boundary element.

In this study, for a more accurate calculation, the drag force as viscous damping on the submerged moving body was considered in the frequency domain. Generally, the viscous damping effect cannot be considered in the potential-fluid-based calculation. The equation of motion of the system was set to predict the vertical responses of a floater and submerged body under various wave conditions. The equation incorporated the drag force on the submerged body, which is proportional to the squared velocity, to represent the viscous damping of the corresponding moving submerged body. Linearized viscous damping was applied to the equation of motion using an equivalent linearization scheme.

A range of physical parameters, such as the dimensions of the submerged body and stiffness of the connection line were applied to the equation of motion to determine the optimal conditions for a two-body floating system. To minimize the vertical motion of the floater at the target frequency, the resonance frequency of the heave response amplitude operator (heave RAO) of the floater must be controlled. With various dimensions of the submerged body in addition to the properties of the connection lines, the resonance frequency of a two-body system may be shifted to avoid a certain range of target incident frequencies. This study focused on the control of vertical motion of a floating body because the target structure was a marina structure or floating dock in the harbor or near shore. Therefore, the two-body system was moored by the vertical pile guide, and the system was only allowed to move vertically.

MATHEMATICAL FORMULATIONS

1. Basic theory background

The equation of vertical motion of a floating structure is expressed as

$$(M + A)\ddot{x}_3 + C\dot{x}_3 + \rho g A_W x_3 = F, \quad (1)$$

where *M, A, C, ρ, g, A_w,* and *F* are the body mass, heave added mass, radiation damping coefficient, water density (= 1025 kg/m^3), gravitational acceleration (= 9.81 m/s^2), water-plane area of the body, and excitation force, respectively. x_3, $\dot{x}_3$, $\ddot{x}_3$ denote vertical displacement, velocity, and acceleration of the body, respectively.

This study considered a floater and a submerged body connected via a connection line, which is expressed as the added stiffness. The two-degrees-of-freedom equation of vertical motion is modeled as follows:

$$\begin{cases} (M_{33} + A_{33})\ddot{x}_3 + C_{33}\dot{x}_3 + K_{33}x_3 + K_{added}x_3 \\ \qquad - K_{added}x_9 + A_{39}\ddot{x}_9 + C_{39}\dot{x}_9 = F_3 e^{i\omega t} \\ (M_{99} + A_{99})\ddot{x}_9 + C_{99}\dot{x}_9 + K_{99}x_9 + K_{added}x_9 \\ \qquad - K_{added}x_3 + A_{93}\ddot{x}_3 + C_{93}\dot{x}_3 = F_9 e^{i\omega t} \end{cases} \quad (2)$$

Here, subscripts three and nine represent the vertical direction of the floater and submerged body, respectively. K_{added} is the added stiffness of a connection line with the unit length.

The movement of the floater and submerged body, in addition to the wave force on the body, are assumed to be harmonic in the frequency domain. Therefore, the motion and force are expressed as follows:

$$x_j = X_j e^{i\omega t}, \quad (3)$$

$$\text{Excitation Force} = F_j e^{i\omega t}, \quad (4)$$

where j equals three or nine. Applying Eq. (3) and (4), Eq. (2) can be expressed in matrix form, as shown below, to model a two-degrees-of-freedom system.

$$\begin{bmatrix} -\omega^2(M_{33}+A_{33}) + K_{33} + K_{added} + i\omega C_{33} & -\omega^2 A_{39} - K_{added} + i\omega C_{39} \\ -\omega^2 A_{93} - K_{added} + i\omega C_{93} & -\omega^2(M_{99}+A_{99}) + K_{99} + K_{added} + i\omega C_{99} \end{bmatrix} \begin{bmatrix} X_3 \\ X_9 \end{bmatrix} = \begin{bmatrix} F_3 \\ F_9 \end{bmatrix}, \quad (5)$$

where K_{99} is zero owing to the no-water-plane area of the submerged body.

With radiation damping, the coupled terms and the excitation force acting on the submerged body are small, and the response of a floater can be calculated using the following equation:

$$X_3 = \frac{F_3\{-\omega^2(M_{99}+A_{99}) + K_{added}\}}{\{-\omega^2(M_{33}+A_{33}) + K_{33} + K_{added}\}\{-\omega^2(M_{99}+A_{99}) + K_{added}\} - K_{added}^2}. \quad (6)$$

Therefore, the vertical displacement of a floater (X_3) can be minimized at a certain incident wave frequency. The wave frequency is $\omega_{\min}$, as determined in Eq. (7).

$$\omega_{\min} = \sqrt{\frac{K_{added}}{(M_{99}+A_{99})}}, \quad \text{where } K_{added}(=K_a) = \frac{EA_{line}}{L} \quad (7)$$

E, A_{line}, and L are the elastic modulus, cross-sectional area, and length of the connection line, respectively. Specifically, the heave RAO of the floater can be minimized if the connection line stiffness and submerged body dimensions are regulated properly. This forms the fundamental concept of the present study.

2. Drag force on a submerged body

As the submerged body moves vertically in the water, the viscous damping (or drag) force acts as an additional force on the body. Therefore, the drag force on the submerged body is provided as follows:

$$F_D = \frac{1}{2}\rho C_D A_S \dot{x}_9 |\dot{x}_9| = C_{Drag}\dot{x}_9 |\dot{x}_9|, \quad (8)$$

where C_D and A_S are the drag coefficient of a submerged body and its projected area for the vertical motion, respectively. C_{Drag} was set to $0.5\rho C_D A_S$.

According to the Det Norske Veritas (DNV) rule (2011), the drag coefficient (C_D) was selected as 1.2 for a three-dimensional rectangular plate in the case of normal directional flow and a Reynolds number greater than 10^3 ($\mathrm{Re} > 10^3$).

When a nonlinear drag force (Eq. 8) is applied to a linear frequency domain calculation, the drag force must be transformed to an equivalent linear damping term using the linearization of nonlinear damping. This linearization is established based on the following fact: energy (i.e., work done per unit time) dissipated by the radiated wave and viscous damping is equal to the energy dissipated by an equivalent linear damping coefficient. This concept is expressed as

$$C_{eq} = C_{99} + \frac{8}{3\pi}\omega |x_9| C_{Drag}, \quad (9)$$

where ω, C_{99}, and C_{eq} denote the wave frequency, heave radiation damping coefficient of a submerged body, and equivalent linear damping coefficient, respectively. To calculate the equivalent linear damping coefficient (C_{eq}), the vertical velocity of the submerged body ($|\dot{x}_9|$) needs to be updated implicitly. The equivalent linear coefficient was determined through an iterative process. The equation of the two-degrees-of-freedom system motion was rearranged and its final form is presented as follows:

$$\begin{cases} (M_{33}+A_{33})\ddot{x}_3 + C_{33}\dot{x}_3 + K_{33}x_3 + K_{added}x_3 - K_{added}x_9 + A_{39}\ddot{x}_9 + C_{39}\dot{x}_9 = F_3 e^{i\omega t} \\ (M_{99}+A_{99})\ddot{x}_9 + C_{eq}\dot{x}_9 + K_{added}x_9 - K_{added}x_3 + A_{93}\ddot{x}_3 + C_{93}\dot{x}_3 = F_9 e^{i\omega t} \end{cases} \quad (10)$$

If the body motion and wave force are assumed to be harmonic, Eq. (10) then becomes a matrix, which is expressed as

$$\begin{bmatrix} -\omega^2(M_{33}+A_{33}) + K_{33} + K_{added} + i\omega C_{33} & -\omega^2 A_{39} - K_{added} + i\omega C_{39} \\ -\omega^2 A_{93} - K_{added} + i\omega C_{93} & -\omega^2(M_{99}+A_{99}) + K_{added} + i\omega C_{eq} \end{bmatrix} \begin{bmatrix} X_3 \\ X_9 \end{bmatrix} = \begin{bmatrix} F_3 \\ F_9 \end{bmatrix}. \quad (11)$$

Using Cramer's rule, the responses of the floater (X_3) and submerged body (X_9) can be calculated. In particular, the response of the floater can indicate a local minimum at certain incident wave frequencies. For practical applications, such as marina structures, only vertical motion of the two-body system was considered in this study, and other motions, such as surge and pitch were not investigated.

NUMERICAL RESULTS

Fig. 1 illustrates the numerical model and presents a schematic diagram of the two-degrees-of-freedom system. The numerical model consists of a floater and a submerged body with a connection line, which is defined as additional stiffness represented by a spring constant. The floater was 5 m in length, 2 m in width, and 0.5 m in draft (L = 5 m, B = 2 m, and D_T = 0.5 m). The total number of calculation nodes for grid generation of the floater and submerged body were 909 and 572, respectively. All hydrodynamic analyses in this study were based on the beam sea conditions, which equate to the severest wave conditions. Table 1 provides details of the calculation conditions discussed here.

To reduce the vertical motion of the floater (upper body), two parameters of the two-body system must be regulated: dimensions of the submerged body and stiffness of the connection line.

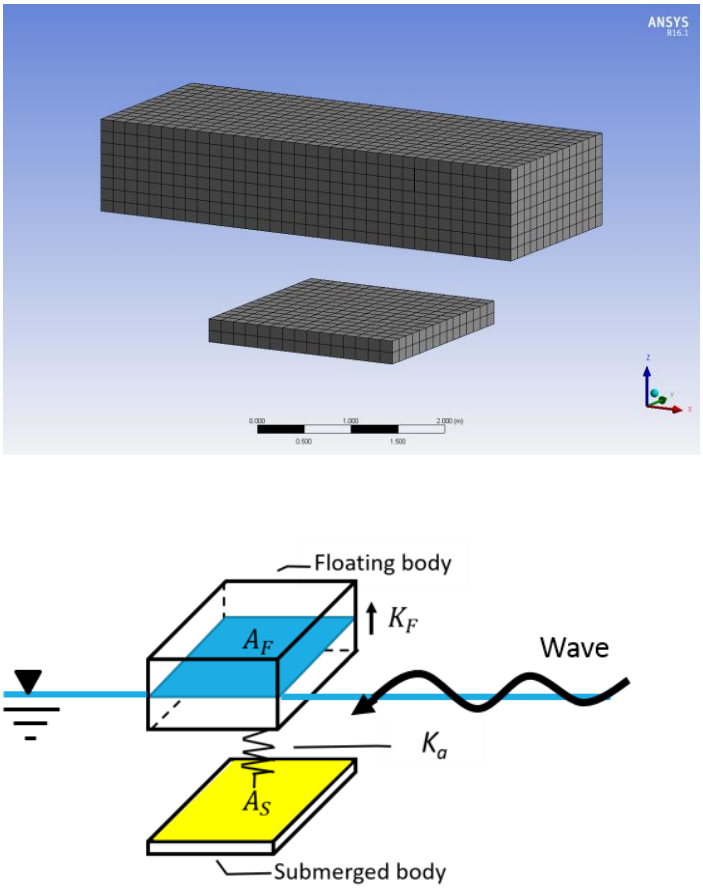

Figure 1. Numerical model and schematic diagram of the two-degrees-of-freedom system.

The vertical stiffness of the connection line is provided as $K_a = EA_{line}/L$, where E is the elastic modulus of the line (0.7 MPa for rubber), and A_{line} is the cross-sectional area. Because the length of the connection line (L) was selected as the unit length in this study, the stiffness of the line can vary

according to the cross-sectional area and material properties. The projected area of the submerged body (A_S) may act as an additional significant factor in regulating the vertical motion of a floater because the body dimensions have significant effects on the drag force and added mass.

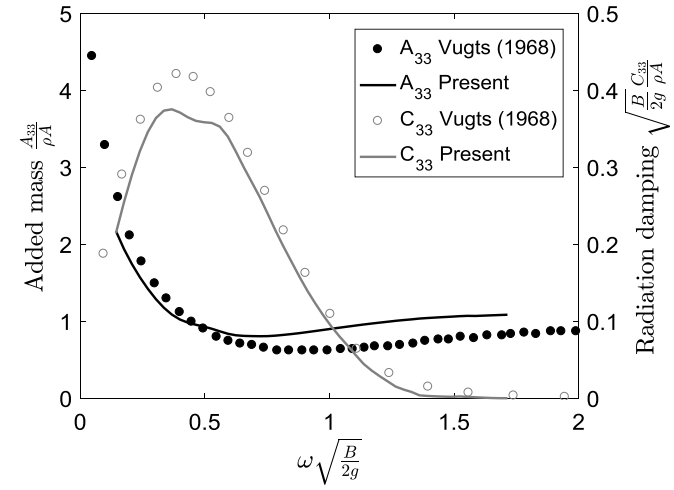

(a)

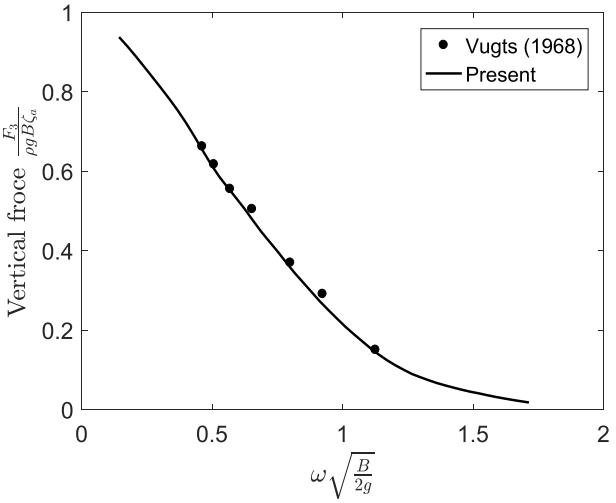

(b)

Figure 2. Comparison of (a) heave added mass, radiation damping coefficient and (b) excitation force for a 2D rectangular single buoy with the results of Vugts (1968)

To validate the solutions presented in this paper, Fig. 2 shows comparisons of heave added mass, radiation damping and vertical excitation force with the results of Vugts (1968). The present calculations are the results of ANSYS AQWA. The added mass and radiation damping coefficient show reasonable agreement with the results of Vugts (1968), even if the present results retains 3D effects. Moreover, vertical excitation acting on a rectangular single buoy fairly agrees with Vugts (1968).

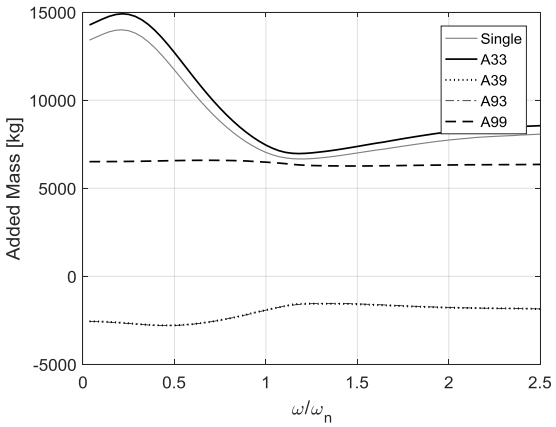

(a)

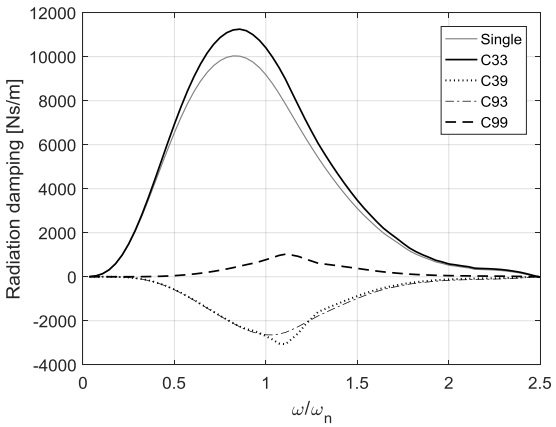

(b)

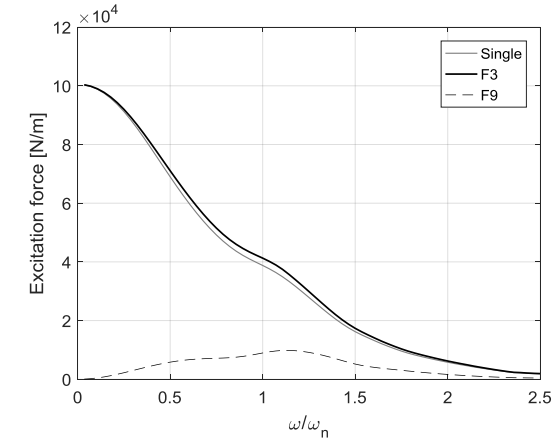

(c)

Figure 3. Comparison of (a) heave added mass, (b) radiation damping coefficient including coupled terms and (c) excitation force for Single and floater-submerged body

Fig. 3 shows heave added mass, radiation damping coefficient and excitation force of floater-submerged body including coupled terms whose subscripts are 39 and 93. The radiation force and excitation force were obtained by using hydrodynamic commercial software (AQWA). The radiation force involving added mass and radiation damping coefficient

could be obtained by solving a problem with a forced oscillating buoy in calm water. The diffraction force could be computed with a constraint buoy condition under incident waves.

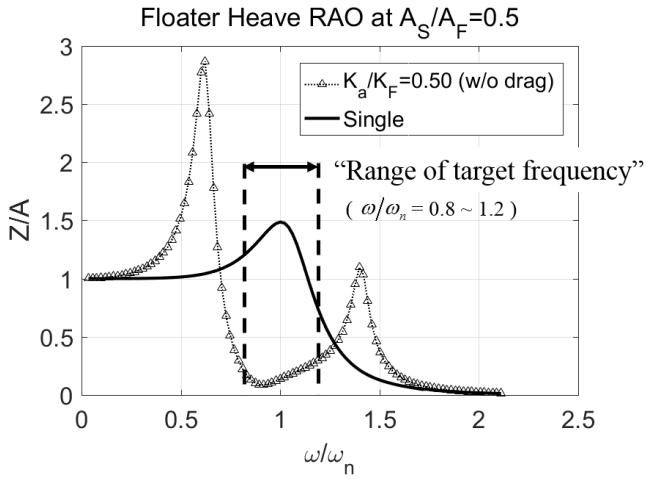

Figure 4. Single body and two-body system comparison of the floater heave RAOs. A_S/A_F = 0.5 and K_a/K_F = 0.50.

Fig. 4 compares the heave RAOs for a single floater and a floater in a two-body system. The heave RAO of the body decreases significantly at the resonance frequency when a two-body system is applied to the floater; the resulting heave RAO of the two-body system is approximately 80% less than that of the single body. Two resonance frequencies are observed because of the two-degrees-of-freedom system. The first (primary) resonance frequency originates from the natural frequency of the single body, and the secondary resonance frequency is generated from the two-body interaction with the connection line. The viscous damping on the submerged body was not considered in this case. Furthermore, the ratio between the projected area of the submerged body and the floater (A_S/A_F) is 0.5. The ratio between the vertical stiffness (K_a) of the connection line and heave restoring coefficient (K_F) of the floater is 0.5. The dimensions of the floater in the two-body system are the same as the single body, and the submerged body is assumed to be neutrally buoyant.

The target frequency for reducing the vertical motion of the floater is selected as a frequency near the resonance frequency of a single-body floater. In this study, the range of the target frequency was 0.8~1.2 times the natural frequency of a single-body floater.

Five varying ratios of vertical projected areas (A_S/A_F) were considered to evaluate the response of a floater in waves. The added stiffness (K_a) of the connection line (unit length) was varied according to the material properties and the cross-sectional area of the line. The stiffness (K_a) ranged from 0.05 to 1.37 times that of the restoring coefficient of the floater ($K_{33} = K_F$); furthermore, a total of 18 varying ratios of K_a/K_F were considered.

Table 1. Numerical model details

	Item	Dimension
Floater	$L \times B \times D_T$	$5\ m \times 2\ m \times 0.5\ m$
	Water-plane area A_F (= $L \times B$)	$10\ m^2$
	Mass (M_{33})	5,125 kg
	Vertical restoring coefficient, $K_{33}(=K_F)$	$1.0 \times 10^5\ N/m$
Submerged body	Mass (M_{99})	1,281.25 kg
	Area, A_S	$0.1A_F$, $0.2A_F$, $0.3A_F$, $0.4A_F$, $0.5A_F$ (Total 5 cases)
Connection line	Added stiffness, $K_a(=K_{added})$	$0.05K_F$ ~ $0.90K_F$ (0.05 interval), and $1.37K_F$ (Total 18 cases)
Incident wave	Frequency, ω	$0.1 \sim 6.0$ rad/s (100 cases, $\Delta\omega = 0.06$ rad/s)

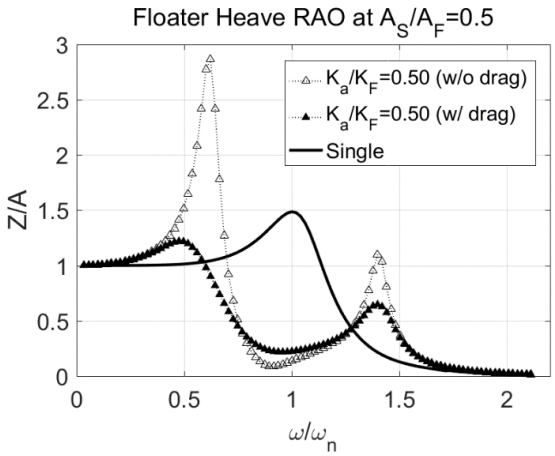

Figure 5. Drag effects on the floater heave reduction. A_S/A_F = 0.5 and K_a/K_F = 0.50.

In general, the magnitude of the heave RAO may decrease with additional viscous damping. Therefore, the enhanced accuracy of the floater heave RAO in a two-body system can be achieved by applying a drag force to the submerged moving body.

Fig. 5 presents the drag effects of the submerged body on the floater heave reduction. The magnitude of the heave RAO shows a significant decrease with regard to the primary and secondary resonance frequencies. The drag coefficient may vary according to the shape of the submerged body and the KC number. In this study, the coefficient of the submerged rectangular body (C_D) is selected as 1.2, which was determined from the DNV rules, and its value was applied to Eq. (8).

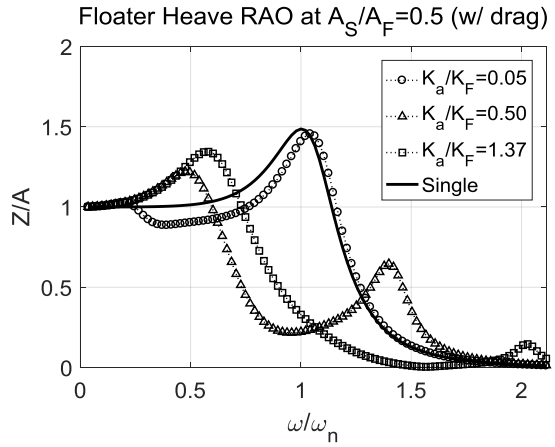

(a)

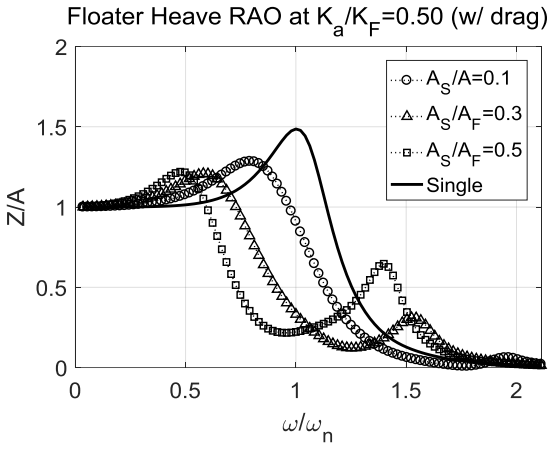

(b)

Figure 6. Comparison of the heave RAOs of the floater for various A_S/A_F and K_a/K_F (ω_n is the natural heave frequency of a single body).

Fig. 6 shows the representative heave RAOs of the floater for given ratios of the area of the submerged body and the floater, and connection stiffness, respectively. The secondary resonance frequency varies according to the dimensions of the submerged body and the stiffness of the connection line. Moreover, the first resonance frequency fluctuates according to the secondary resonance frequency.

In Fig. 6(a), when the added stiffness of the connection line is relatively lower (K_a/K_F = 0.05), the primary resonance frequency of the floater heave RAO is comparable to that of the single body (ω/ω_n = 1). In addition, the secondary natural frequency is a lower frequency than the natural frequency of the single body. As the stiffness of the connection line increases, the secondary natural frequency shifts to a high frequency. Therefore, the two natural frequencies are observed clearly when K_a/K_F = 0.5.

In Fig. 6(b), the primary resonance frequency decreases with increasing area of the submerged body. Therefore, as the added mass of the submerged body increases (i.e., when the area of the submerged body is relatively larger), the secondary resonance frequency of the floater RAO shifts to a lower frequency.

Through this comparison, it is apparent that the value of the primary and secondary resonance frequency can vary according to the dimensions of the submerged body and the added stiffness of the connection line. At the target frequency, i.e., the resonance frequency of the single body, the heave RAO of the floater is shown to exhibit a significant decrease resulting from a shift in the resonance frequency. The heave RAO exhibited an additional increase both above and below the corresponding value of the single-body natural frequency.

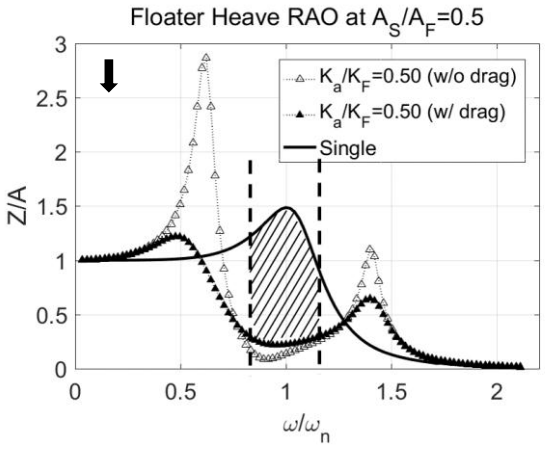

(a)

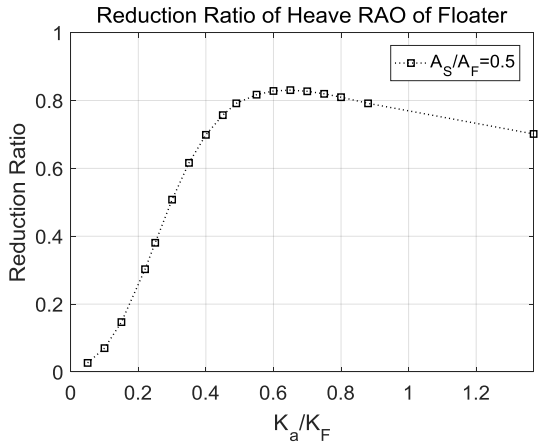

(b)

Figure 7. Reduction ratio of the floater heave RAO for A_S/A_F = 0.5 and K_a/K_F = 0.5. The hatched area is the target frequency range. The arrow in (b) corresponds to the case of (a).

The reduction ratio is a non-dimensional parameter for the heave RAO decrement of the floater due to two-body interaction. The ratio is calculated for the range of target frequencies, as shown in Fig. 5 (ω/ω_n = 0.8~1.2).

$$\text{Reduction Ratio} = \int_{\omega/\omega_n=0.8}^{1.2} \frac{\text{Heave RAO of a single body - Heave RAO of the floater in 2 DOF system}}{\text{Heave RAO of a single body}}$$

Fig. 7 (a) shows the reduction of the heave RAO resulting from two-body interaction, as determined in this study. The hatched area characterizes the magnitude of the heave reduction within the target frequency. Fig. 7 (b) presents the reduction ratio for A_S/A_F = 0.5 for various ratios of connection line stiffness; the arrow corresponds to the illustration in Fig. 7 (a).

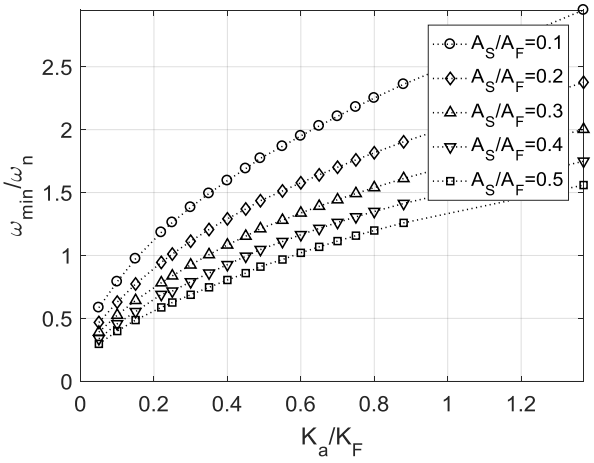

Figure 8. Non-dimensional natural frequency of the submerged body for various A_S/A_F and K_a/K_F. Floater dimensions are as shown in Table 1.

Predicting the frequency for the minimum heave RAO of a floater in a two-body system in the absence of detailed numerical analyses is generally difficult. Therefore, a prediction of the heave reduction should incorporate another parameter related to the submerged body in the system. As the natural frequency of a submerged body, $\omega_{\min}$ can be calculated by $\sqrt{K_{added}/(M_{99}+A_{99})}$, the floater heave reduction in a two-body system should be presented as a function of $\omega_{\min}$.

Fig. 8 shows the non-dimensional natural frequency ($\omega_{\min}/\omega_n$) for all connection stiffness and vertical projected areas. The $\omega_{\min}$ increases gradually as the added stiffness increases with decreasing submerged body area.

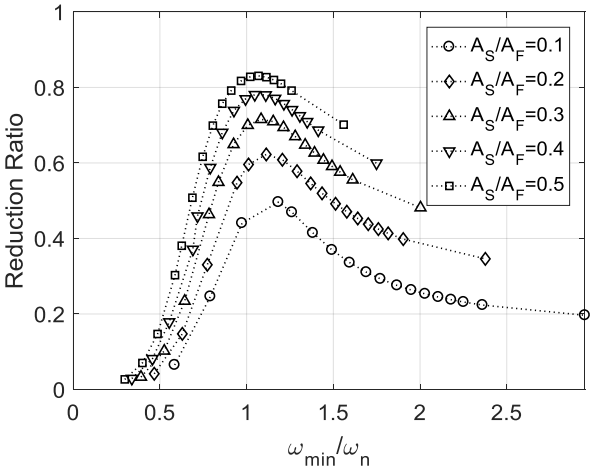

Figure 9. Floater heave reduction ratio in the two-body system with viscous damping on the submerged body (floater dimensions are shown in Table 1).

Fig. 9 compares the reduction ratios for the floater heave RAO for all the computational cases presented in this study. The ratio is presented as a function of the natural frequency of the submerged body. The maximum heave reduction is observed to occur when $\omega_{\min}/\omega_n \approx 1.1$, which corresponds to the natural frequency of the submerged body being 10% higher than that of the single floating body. In particular, the reduction ratio can exceed 80% when the ratio of the vertical projected area (A_S/A_F) is 0.5.

Consequently, to maximize the heave reduction of a floating structure connected to a submerged body in a two-body system, the natural frequency of the submerged body should be approximately 10% greater than that of the target single floating body structure ($\omega_{\min}/\omega_n \approx 1.1$). Furthermore, under the optimal frequency condition, the reduction ratio increased with increasing area ratio.

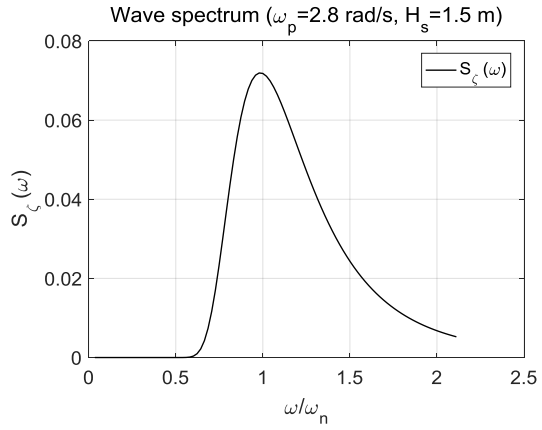

(a)

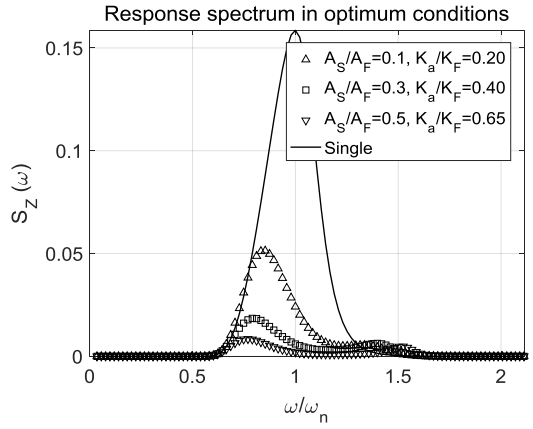

(b)

Figure 10. Incident wave spectrum (PM spectrum) and response spectra under the optimal conditions. H_S =1.5 m, ω_p =2.8 rad/s

Under irregular wave conditions, the PM spectrum was used as the incident wave condition to calculate the vertical motion of a floater. The PM spectrum can be expressed as

$$S_\zeta(\omega) = \frac{5}{16} H_S^2 \omega_p^4 \omega^{-5} e^{-1.25\left(\frac{\omega_p}{\omega}\right)^4}, \quad (12)$$

where H_S and ω_p denote the significant wave height and peak frequency, respectively. The response spectra of the floater (Eq. 13) can be calculated using the RAO and wave spectrum. The significant heave amplitude of the floater (Eq. 14) can be determined from the response spectra.

$$S_Z(\omega) = \left|\frac{Z}{A}(\omega)\right|^2 S_\zeta(\omega) \quad (13)$$

$$Z_{1/3} = 2\sqrt{\int_0^\infty S_Z(\omega)\, d\omega} \quad (14)$$

Fig. 10 presents the incident wave spectrum and response spectra of the floater. The peak wave frequency is the resonance frequency of the single body floater ($\omega_p = 2.8$ rad/s), which was the target frequency in this study. The significant wave height ($H_{1/3}$) was set to 1.5 m. Generally, the heave reduction ratio is not affected by the significant wave height. Fig. 10 (b) compares the response spectra of the floater under the optimal conditions of regular wave analysis in Fig. 9. The heave response of the floater in irregular waves decreases significantly as the area of the submerged body increases. The response spectra can be reduced greatly due to the influence of the square of the heave RAO.

Table 2. Significant heave amplitude of the floater

	$Z_{1/3}$ (m)	Reduction (%)
Single	0.73	-
$A_S/A_F = 0.1$	0.42	42.3
$A_S/A_F = 0.3$	0.28	62.2
$A_S/A_F = 0.5$	0.19	73.7

Table 2 lists the significant heave amplitude obtained from the response spectra in Fig. 10 (b). The significant heave amplitude of the floater decreases considerably as the area of the submerged body increases. The maximum reduction by 73.7% was observed under the condition of $A_S/A_F = 0.5$ in this study.

CONCLUSIONS

This paper presented a numerical study of the effect of submerged body to reduce the vertical movement of a floater via a two-body interaction system that incorporated various body dimensions and connection conditions. Two resonance frequencies were evident in the two-degrees-of-freedom system.

Two parameters, vertical projected area of the submerged body and connection line stiffness, were considered to analyze the fluctuations in the primary and secondary resonance frequencies associated with the vertical responses of the floater. Therefore, the heave RAO of the floater exhibited a significant decrease in the range of target frequencies due to the two-body interactions. Moreover, when the viscous damping effect of the submerged body was applied, the magnitude of the heave RAO at both resonance frequencies decreased considerably.

The floater heave reduction can also be analyzed by observing the heave reduction ratio as a function of the submerged body natural frequency ($\omega_{\min}$). The maximum heave reduction occurred when $\omega_{\min}$ was approximately 10% higher than that of the single floating body ($\omega_{\min} / \omega_n \approx 1.1$) under regular wave conditions. In this case, the heave reduction ratio exceeded 80% when the ratio of the vertical projected area (A_S / A_F) was 0.5.

Under irregular wave conditions, the heave response spectra and significant amplitude of the floater decreased significantly as the area of the submerged body increased. The significant heave amplitude of the floater decreased up to 73.7% under the condition of $A_S / A_F = 0.5$ in this study.

These results may provide the basis for developing two-body floating systems with regard to designing the submerged body such that the vertical motion of the floater is minimized. To achieve a practical design of a two-body floating system, it is essential to investigate the drag coefficient for various shapes of the submerged body, in addition to using the proper materials for connection lines to modulate the floater motion.

ACKNOWLEDGMENT

This research was a part of the project titled, “Manpower training program for ocean energy” funded by the Ministry of Oceans and Fisheries, Korea. This research was supported by Basic Science Research Program through the National Research Foundation of Korea (NRF), funded by the Ministry of Science, ICT & Future Planning (2015R1D1A1A01057769). This work was additionally supported by the Korea-UK Global Engineer Education program for Offshore Plants by the Ministry of Trade, Industry, and Energy Affairs (MOTIE).

REFERENCES

[1] An, S., and Faltinsen, O.M., 2013, "An experimental and numerical study of heave added mass and damping of horizontally submerged and perforated rectangular plates", J. Fluids and Structures, 39, pp. 87-101.

[2] Cozijn, H., Uittenbogaard, R., and Brake, E., 2005, "Heave, Roll and Pitch Damping of a Deepwater CALM Buoy with a Skirt," Proc. 15th International Offshore and Polar Engineering Conference, Seoul, Korea, pp. 388-395.

[3] Engstrom, J. Kurupath, V., Isberg, J., and Leijon, M., 2011, "A resonant two body system for a point absorbing wave energy converter with direct-driven linear generator," J. applied physics, 110, 124904.

[4] Geng, B., Teng, B., Zhang, H., and Zheng, B., 2012, "Viscous Damping Effect on the First Order Motion Response of a Truss Spar," J. Shipping and Ocean Eng., 2 , pp. 100-106.

[5] Journée, J. M. J. and Massie, W. W., 2001, Offshore Hydromechanics, Ch 6. Rigid body dynamics.

[6] Modelling and Analysis of Marin Operation, 2011, Recommended Practice DNV-RP-H103, APPENDIX B Drag coefficient, pp. 143-148.

[7] Shen, W. J., Tang, Y. G., and Liu, L. G., 2012, "Research on the Hydrodynamic Characteristics of Heave Plate Structure with Different Form Edges of a Spar Platform," Chinese Ocean Eng., 26(1), pp. 177-184.

[8] Tarrant, K. and Meskell, C., 2016, "Investigation on parametrically excited motions of point absorbers in regular waves," Ocean Eng., 111, pp. 67-81.

[9] Tao, L. B. and Cai, S. G., 2004, "Heave motion suppression of a Spar with a heave plate," Ocean Eng., 31, pp. 669-692.

[10] Tao, L., Molin, B., Scolan, Y.-M., and Thiagarajan, K., 2007. "Spacing effects on hydrodynamics of heave plates on offshore structures," J. Fluid and Structures, 23, pp. 1119-1136.

[11] Li, J., Liu, S., Zhao, M., and Teng, B., 2013, "Experimental investigation of the hydrodynamic characteristics of heave plates using forced oscillation," Ocean Eng., 66, pp. 82-91.

[12] Li, Y, Yu, Y. H., Epler, J., and Previsic, M., 2012, "Experimental Investigation of the power generation performance of floating-point absorber wave energy systems," Proc. 27th International workshop on water waves and Floating Bodies, Copenhagen, Denmark.

[13] Vugts, Ir. J. H., 1968, "The Hydrodynamic coefficients for swaying, heaving and rolling cylinders in a free surface," Netherlands Ship Res. Centre TNO. Report No. 194. Delft: Shipbuilding Lab., Delft University of Technology.